MODELING OF TURBULENT FLOWS WITH A SURFACE-PLACED OBSTACLE AND A LINE SOURCE OF PASSIVE SCALAR

Albert F. Kurbatskii [1,2] and Sergey N. Yakovenko [1,2]
[1] Department of Physics, Novosibirsk State University
630090 Novosibirsk, Russia
[2] Laboratory of Turbulence Modelling, Institute of Theoretical and Applied Mechanics,
Russian Academy of Sciences, Siberian Branch,
630090 Novosibirsk, Russia

ABSTRACT

Results of modeling a turbulent flow around a two-dimensional surface-placed obstacle of square cross-section have been obtained. Possibilities of algebraic and differential second-order models have been studied for the cases of a channel flow with a rib and turbulent boundary layer on a plate with a line source of passive contaminant. Scalar diffusion from the source in a flow behind a backward-facing step and in the boundary layer with the obstacle has been calculated.

INTRODUCTION

Complex turbulent flows are accompanied by processes of separation and reattachment because of sharp edges of bodies situated in a flow. A local step to solve a general problem of adequate description of such phenomena is to develop a model for a flow with a surface-placed quadratic obstacle.

Recent years two-dimensional flows with sharp-edged boundaries have been studied intensively both experimentally and theoretically. The noticeable progress has been achieved in description of a flow behind a backward-facing step, e.g. in (Laurence et al., 1997; Craft, 1997) due to detailed base of data of experiments (e.g. (Driver and Seegmiller, 1985)) and DNS (Le et al., 1997). A flow around an obstacle is more serious test for experimental device, turbulence model and numerical procedure owing to (caused by a windward corner) sharper change of pressure, velocity and larger increase of turbulent intensities in the thin layer on the obstacle top. A number of computations mainly by the k-ε model has been realized for a single two-dimensional rib in channels (e.g. (Durst and Rastogi, 1979; Benodekar et al., 1985)), for a cube (e.g. (Murakami and Mochida, 1988)). Despite an agreement with measured distributions of mean velocity in the whole, some flow features (in particular, recovery after reattachment and behavior of turbulent intensities) were not predicted adequately. The present paper contains results of computations of a flow with the obstacle using Reynolds-stress models (RSM) of different closure level and concentrates in description of flow characteristics near the obstacle where recirculation zones are formed.

Diffusion of matter and heat is of primary importance in industrial, chemical and atmospheric studies. As it is known, a shortcoming of the gradient diffusion model for turbulent fluxes of matter is that it is a local model. However, because of its simplicity the K-theory remains an attractive approximation due to that it provides acceptably accurate results in a number of applications. The present paper includes results of concentration field prediction for flows with flat and sharp-edged boundaries and line sources of passive contaminant.

VELOCITY FIELD IN A FLOW WITH AN OBSTACLE

The Reynolds-averaged Navier–Stokes equations are used to compute the mean velocity and pressure fields in flows with the quadratic cross-section obstacle of height H (in the boundary layer of thickness $\delta >> H$ and in the plane channel of height $2H$). The velocity and length scales of the boundary layer flow are chosen as in the experiments of Murakami and Mochida (1988) with the Reynolds number $\mathrm{Re}_H = 7 \cdot 10^4$ based on H and inflow velocity U_H at this height. Details of boundary conditions, equations discretization, computation procedure and results of computation by the k-ε model of the boundary layer with the obstacle are given by Kurbatskii and Yakovenko (1996). The non-uniform meshes 1,2,3,4,5 have the interval d chosen in successive runs to be equal to $H/6$, $H/12$, $H/24$, $H/48$, $H/96$ near the rib. For the boundary layer, computations show convergence of the recirculation regions length with growth of H/d (Fig.1) and at $d = H/48$ give exactly the measured size $x_R/H = 6.8$ (Logan and Phataraphruk, 1989) of rear recirculation zone. Striving for convergence of calculated profiles with grid refinement for a channel flow can be seen in Fig.2 (meshes 2–5) and in Fig.5 (meshes 4,5).

The channel flow has been chosen to test applicability of turbulence models with the help of experiment data of Durst and Rastogi (1979) (Fig.2–5). Differential model (DM) following to that of Launder et al. (1975) contains the transport equation for the Reynolds stress tensor $\langle u_i u_j \rangle$. The non-linear explicit algebraic model (AM) for $\langle u_i u_j \rangle$ reduced from DM (Kurbatskii and Yakovenko, 1998) includes complex function G instead of the constant C_μ in the isotropic coefficient of eddy viscosity used in the linear Boussinesq model (BM).

BM gives negative non-physical values of the horizontal component $\langle u^2 \rangle$ of turbulence energy (Fig.3). The non-linear algebraic model AMN for normal Reynolds stresses is able to reproduce their anisotropy and to correct the shortcoming of BM. The differential model DMN (transport equations for $\langle u^2 \rangle$, $\langle v^2 \rangle$ and linear gradient expression for $\langle uv \rangle$) describes behavior of $\langle u^2 \rangle$ in front of the obstacle, where convection and diffusion processes are essential, better than AMN (Fig.3, at $x/H = -1$). In the whole, DMN and AMN yield close results which are shown only for DMN in Fig.3,4. The complete DM model with the transport equations for all components of the $\langle u_i u_j \rangle$ tensor gives the most exact prediction of the turbulent intensity $\langle u^2 \rangle$ (Fig.3) and mean velocity field (Fig.4) in front of the obstacle, above it and in the recovery region behind it. DM also describes correctly a joint of recirculation zones above the rib and behind it (Fig.5).

The effect of use of various difference schemes for convection terms in the equations for calculation of flows around sharp-edged obstacles at high Reynolds numbers has been examined. In particular, the differences between the results of computation (Fig.5) with the different schemes (e.g. first-order upwind scheme and QUICK) by the same model at the refined grid are much less of discrepancies of sought functions and streamlines calculated by various turbulence models (Fig.3–5) but with the same convection scheme.

SCALAR DIFFUSION FROM LINE SOURCES

Modeling of turbulent diffusion of passive scalar in the boundary layer from a line source of constant mass flux of ammonia situated as in experiments of Poreh and Cermak (1964) has been carried out. The mean concentration $C(x,y)$ of pollutant is defined from the transport equation

$$U_k \frac{\partial C}{\partial x_k} = \frac{\partial}{\partial x_k}\left[\lambda \frac{\partial C}{\partial x_k} - \langle u_k c \rangle\right] \qquad (1)$$

A simple way of determining $\langle u_k c \rangle$ is the gradient K-model $\langle u_k c \rangle = -\lambda_T (\partial C / \partial x_k)$, $\lambda_T = \nu_T / \sigma_T$ with turbulent Prandtl number $\sigma_T = 0.9$. For the boundary layer we retain the term of (1) with the vertical scalar flux $\langle vc \rangle$. The differential $\langle vc \rangle$ equation (D-model) allowing for wall effect is formulated as

$$U\frac{\partial \langle vc \rangle}{\partial x} + V\frac{\partial \langle vc \rangle}{\partial y} = \frac{\partial}{\partial y}\left[\left(\chi + 2C_S \langle v^2 \rangle \frac{k}{\varepsilon}\right)\frac{\partial \langle vc \rangle}{\partial y}\right] -$$

$$-\langle v^2 \rangle \frac{\partial C}{\partial y} - \left[C_{1C} + C'_{1C}\frac{k^{3/2}}{\varepsilon y} + \left(1 + \frac{\lambda}{\nu}\right) f_C\right]\frac{\varepsilon}{k}\langle vc \rangle \qquad (2)$$

where $\chi = (\lambda + 2\nu)/3$, λ and ν are the molecular diffusivity and viscosity, $f_C = \exp\{-(\mathrm{Re}_T/80)^2\}$, $C_S = 0.11$, $C_{1C} = 3.0$, $C'_{1C} = 0.806$. D-model using the rough BM approximation $\langle v^2 \rangle = 2k/3$ or more exact AMN value $\langle v^2 \rangle \approx 0.46k$ produces a worse prediction of near-source behavior of distributions $C(x,y)$ than K-model. The latter describes measured characteristics fairly well (Fig.6–8) due to distributions of U, k, ε, $\langle uv \rangle$ reproduced by the modified k-ε model (formulated identically to that of Nagano and Tagawa (1990)) in good agreement with the data of experiments (Klebanoff, 1955; Gibson et al., 1984) and DNS (Spalart, 1988). The turbulent diffusivity λ_T (Fig.6) obtained from k and ε varies with distance from a source according to Poreh and Cermak (1964).

For more accurate definition of $\langle v^2 \rangle$ in the near-wall layer, the transport equations for the normal stresses with the pressure-strain and dissipation terms approximations suggested by Lai and So (1990) and reproduced correctly asymptotic behavior of these terms in the near-wall layer are applied. Use of BM for shear stress $\langle uv \rangle$ allows to derive in the local balance approximation an explicit algebraic model (near-wall correction of AMN) for the normal Reynolds stresses describing data of experiments and DNS quite good (Fig.9). Differential equations for normal stresses (near-wall correction of DMN) give similar results. D-model (1), (2) with this correction predicts diffusion characteristics in the same good agreement as that of K-model (Fig.7,8) and reproduces also non-monotonic near-wall behavior of $\partial C / \partial y$ (Fig.10) observed by Poreh and Cermak (1964) at first measuring section. K-model does not describe accurately this fine feature.

A flow behind a backward-facing step has been chosen due to available measurements data of Quante and Enteridge presented by Turfus (1988) for passive scalar diffusion in the rear recirculation zone from sources at locations 1 and 2, namely $(x/H, y/H) = (0.08, 0.8)$ and $(2.4, 0.4)$, where $x = 0$ is the step coordinate, $y = 0$ is vertical coordinate of the bottom at outlet, expansion ratio is ER = 1.111, $\mathrm{Re}_H = 8 \cdot 10^4$. The flow rate Q of contaminant through a thin porous tube and the diameter of this tube producing a line source were very small. Therefore we can neglect (Turfus, 1988) by influence of the source on the velocity fields characteristics which can be taken from separate computation without a source realized then by assignment of Q at locations of contaminant emission. The same way has been used in calculation of the plate boundary layer. K-model has been applied to obtain concentration distributions behind the step. Use of more refined models for the turbulent scalar fluxes $\langle uc \rangle$, $\langle vc \rangle$ is restricted by lack of experiments data for unknown terms of the transport $\langle u_k c \rangle$ equation as well as for the fluxes itself.

There is no measured distributions of velocity fields characteristics in (Turfus, 1988) for a flow with scalar sources (such comparison is carried out in one more run (see Fig.11 for example) corresponding to close conditions of the experiments of Driver and Seegmiller (1985) with ER = 1.125 and sufficiently high Reynolds number). In Fig.12,13 results of scalar field computations of Turfus (1988) by the discrete vortex model for defining trajectories of released particles (models 1 and 2 use different values of effective eddy diffusivity) are plotted together with the measurement and present computation results. One can see that in the whole K-model

gives closer agreement with measurements data than that of Turfus (1988) except near-step locations. Grid independence has been checked in calculations at $H/d = 50$ (dash-dot lines) and 100 (dash-dot-dot lines in Fig.13 at $x/H = 1$ and 2).

Results of computation by K-model of scalar propagation from a source situated on the boundary layer ground upstream of an obstacle are presented in Fig.14. Velocity field characteristics are taken from Kurbatskii and Yakovenko (1996). It can be seen that influence of the sharp-edged obstacle is already noticeable at distance $x/H = -5$ from it and continues up to outflow ($x/H = 20$). For considered location of the line source, effects of the rib consist in the substantial (double) increase of the contaminant jet height, in the decrease of concentration level in recirculation zones behind the obstacle and above leeward edge of it, in the resulting lift up from the wall of position y_{max} where $C(x, y_{max}) = C_{max}(x)$.

CONCLUSIONS

Results of modelling the two-dimensional flow around the surface-placed obstacle of quadratic cross-section show that the basic second-order model following to (Launder et al., 1975) is able to improve prediction of the mean velocity field near the rib and in the recovery region of the closed channel flow and also to yield correct turbulent intensities contrary to those obtained by more simple RSM.

D-model with the $\langle vc \rangle$ transport equation and near-wall corrections of RSM as well as the simplified down-gradient diffusion K-model with the low-Reynolds-number k-ε model allow us to obtain fairly realistic predictions of structural features of the concentration field of contaminant emitted from a ground line source. It means in particular that description of atmosphere ability to diffuse pollutant in terms of the eddy diffusivity which depends as in experiments on vertical coordinate and on distance from the source is possible. D-model can give more exact reproduction of fine features of diffusion field both near the source and near rigid surfaces. However, formulation of an adequate second-order model of scalar transfer for flows with sharp-edged obstacles is restricted by lack of experiments data. K-model describes the concentration field in the most part of a complex separated flow and can be used as the first approximation for solving environmental problems and further development of more accurate models of turbulent heat and matter transfer.

ACKNOWLEDGMENTS

The work was supported by the INTAS (Project Reference Number INTAS-OPEN-97-2022).

REFERENCES

Benodekar, R. W., Goddard, A. J. H., Gosman, A. D., and Issa, R. I., 1985, "Numerical prediction of turbulent flow over surface-mounted ribs," *AIAA Journal*, Vol. 23, pp. 359–366.

Craft, T. J., 1997, "Computations of separating and reattaching flows using a low-Reynolds-number second-moment closure," *Proceedings, 11th International Symposium on Turbulent Shear Flows*, Grenoble, Vol. 3, pp. 30-19–30-24.

Driver, D. M., and Seegmiller, H. L., 1985, "Features of a reattaching turbulent shear layer in divergent channel flow," *AIAA Journal*, Vol. 23, pp. 163–171.

Durst, F., and Rastogi, A. K., 1979, "Theoretical and experimental investigations of turbulent flows with separation," *Turbulent Shear Flows 1*. F. Durst et al., ed., Springer-Verlag, Berlin, pp. 208–221.

Gibson, M. M., Verriopoulos, C. A., and Vlachos, N. S., 1984, "Turbulent boundary layer on a mildly curved convex surface. Part 1: Mean flow and turbulence measurements," *Experiments in Fluids*, Vol. 2, pp. 17–24.

Klebanoff, P. S., 1955, "Characteristics of turbulence in a boundary layer with zero pressure gradient," *NACA Report* 1247.

Kurbatskii, A. F., and Yakovenko, S. N., 1996, "Numerical investigation of turbulent flow around two-dimensional obstacle in the boundary layer," *Thermophysics and Aeromechanics*, Vol. 3, No. 2, pp. 137–155.

Kurbatskii, A. F., and Yakovenko, S. N., 1998, "Modeling a turbulent flow in the plane channel with a quadratic cross-section rib," *Proceedings, 9th International Conference on the Methods of Aerophysical Research*, Vol. 1, ITAM, Novosibirsk, pp. 129–134.

Lai, Y. G., and So, R. M., 1990, "On near-wall turbulent flow modelling," *Journal of Fluid Mechanics*, Vol. 221, pp. 641–673.

Launder, B. E., Reece, G. J., and Rodi, W., 1975, "Progress in the development of a Reynolds-stress turbulence closure," *Journal of Fluid Mechanics*, Vol.68, pp. 537–566.

Laurence, D., Parneux, S., and Durbin, P., 1997, "Second moment closure analysis of a DNS backstep flow database," *Proceedings, 2nd International Symposium on Turbulence, Heat and Mass Transfer*, Hanjalic, K., and Peters, T. W. J., ed., Delft University Press, Delft, pp. 341–350.

Le, H., Moin, P., and Kim, J., 1997, "Direct numerical simulation of turbulent flow over a backward-facing step," *Journal of Fluid Mechanics*, Vol. 330, pp. 349–374.

Logan, E., and Phataraphruk, P., 1989, "Mean flow downstream of two-dimensional roughness elements," Transactions of ASME, *Journal of Fluid Engineering*, pp.149–153.

Murakami, S., and Mochida, A., 1988, "3-D Numerical simulation of airflow around a cubic model by means of k-ε model," *Journal of Wind Engineering and Industrial Aerodynamics*, Vol. 31, pp. 283–303.

Nagano, Y., and Tagawa, M., 1990, "An improved k-ε model for boundary layer flows," Transactions of ASME I, *Journal of Fluid Engineering*, Vol. 112, pp. 33–39.

Poreh, M., and Cermak, J. E., 1964, "Study of diffusion from a line source in a turbulent boundary layer," *International Journal of Heat and Mass Transfer*, Vol.7, pp. 1083–1095.

Spalart, P. S., 1988, "Direct simulation of turbulent boundary layer up to $R_\theta = 1410$," *Journal of Fluid Mechanics*, V. 187, pp. 61-98.

Turfus, C., 1988, "Calculating mean concentrations for steady sources in recirculating wakes by a particle trajectory method," *Atmospheric Environment*, Vol. 22, pp. 1271–1290.

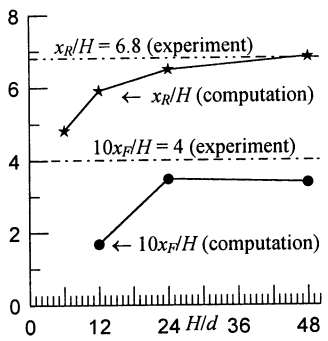

Figure 1. Length of front (x_F) and rear (x_R) recirculation zones.

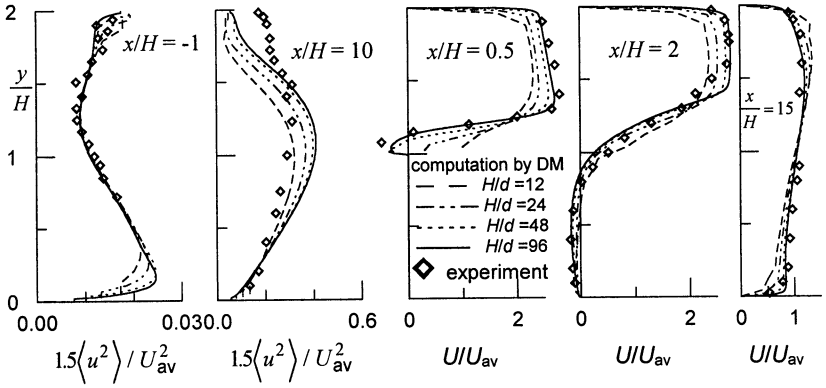

Figure 2. Convergence of profiles with non-uniform grid refinement.

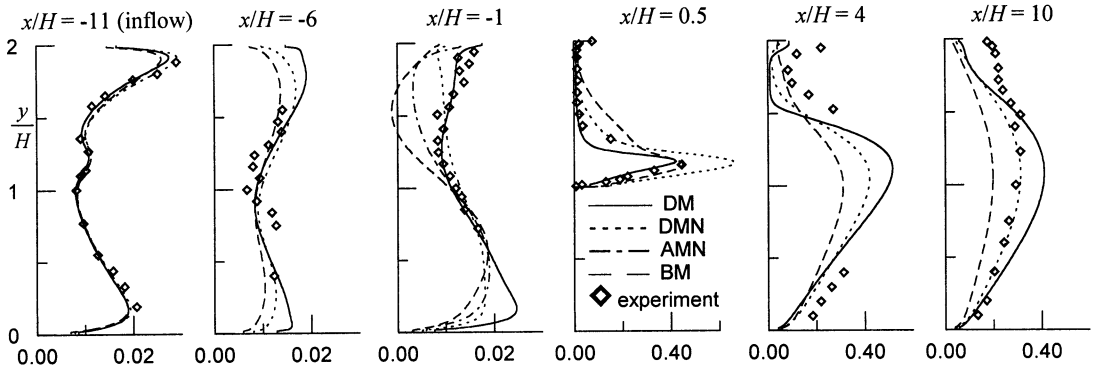

Figure 3. Profiles of horizontal component $1.5\langle u^2\rangle / U_{av}^2$ of turbulence energy in closed channel flow with obstacle.

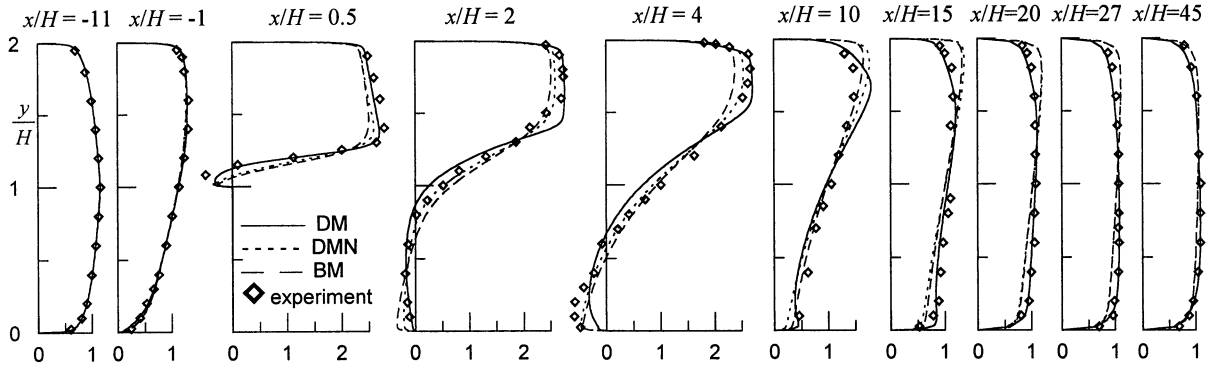

Figure 4. Profiles of mean velocity U/U_{av} in channel flow with obstacle (U_{av} is velocity averaged over cross section).

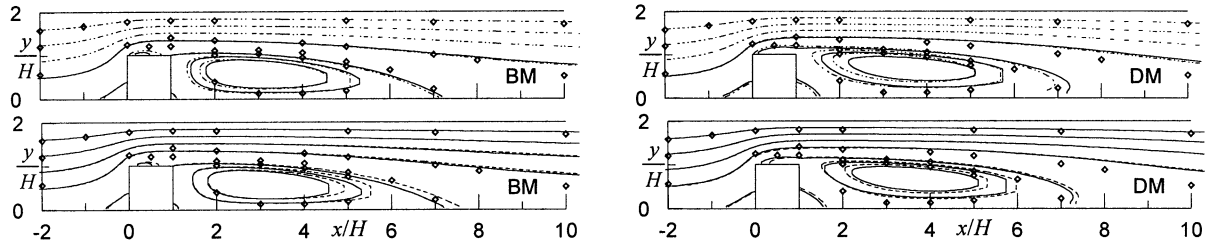

Figure 5. Streamlines obtained in experiments (◇) and computations (- - - - - at H/d = 96; ——— at H/d = 48 with upwind convection scheme; ---------- with second-order convection scheme in equations for U and V).

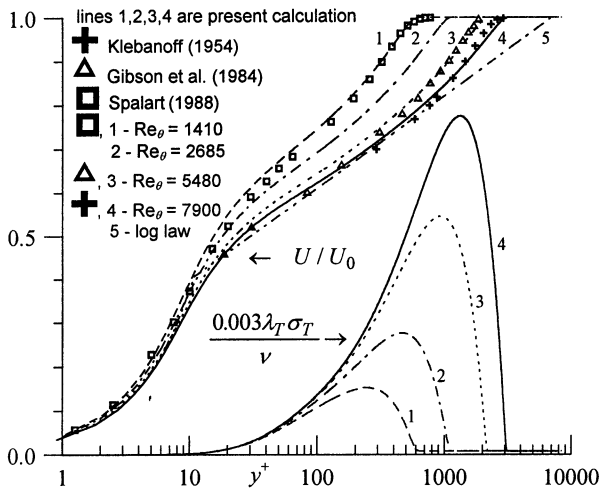

Figure 6. Profiles of mean velocity and turbulent diffusivity.

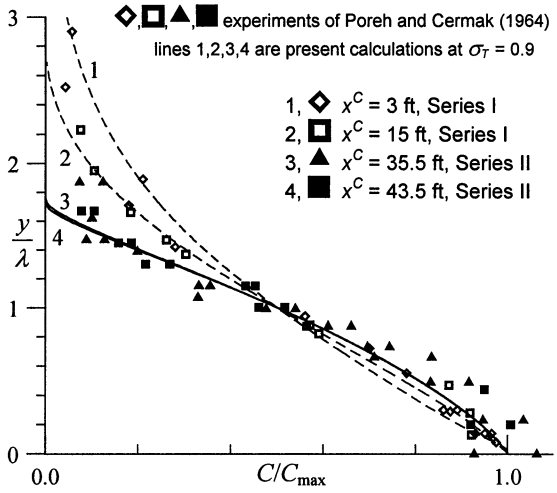

Figure 7. Profiles of mean concentration of scalar.

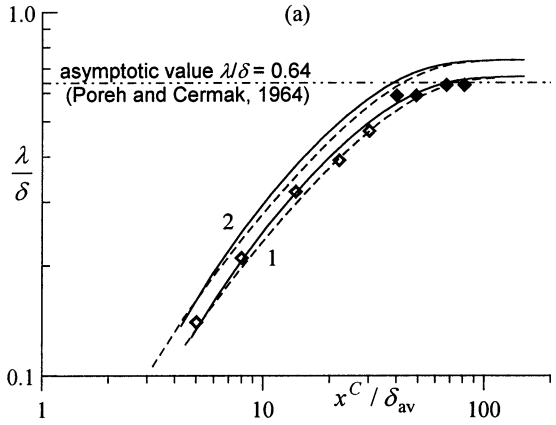

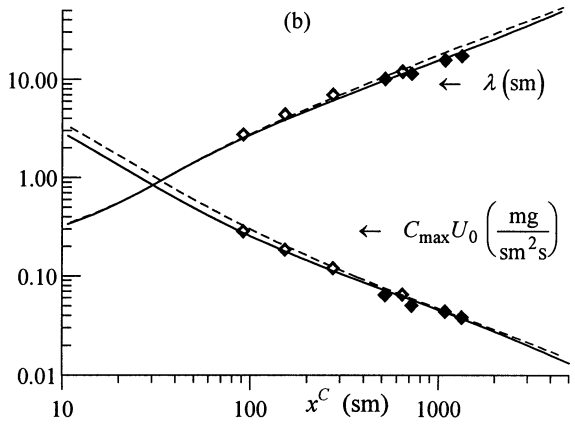

Figure 8. Integral characteristics of diffusion (x^C is distance from the source placed at x = 33.5 ft downstream of the boundary layer origin in Series I and at x = 15.5 ft in Series II; ◇,◆ measurements of Poreh and Cermak (1964); lines are present calculations; ◇, ------ Series I ; ◆, ——— Series II): (a) the ratio λ/δ with a non-dimensional distance from the source (1 - σ_T = 0.90, 2 - σ_T = 0.72); (b) values of half-height λ of a scalar plume and maximum concentration C_{max} (σ_T = 0.90); U_0 is external flow velocity, δ is boundary layer thickness ($U(x, y=\delta) = 0.99U_0$).

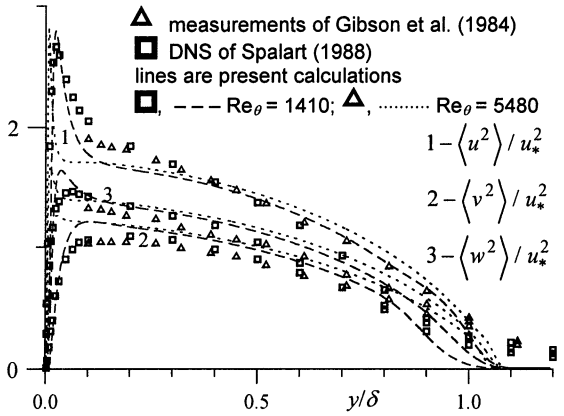

Figure 9. Reynolds stresses in a boundary layer, Re$_\theta$ is Reynolds number based on momentum thickness θ.

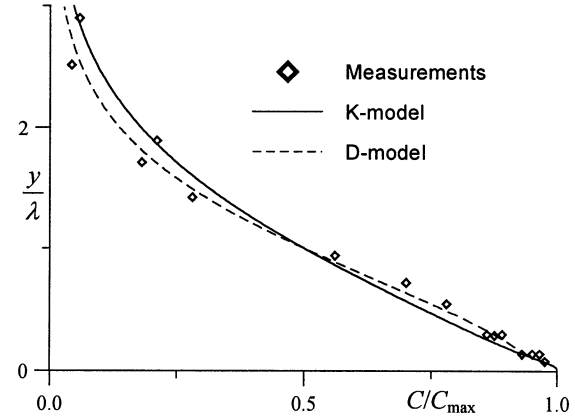

Figure 10. Profiles of normalized mean concentration at distance x^C = 3 ft from a source (Series I).

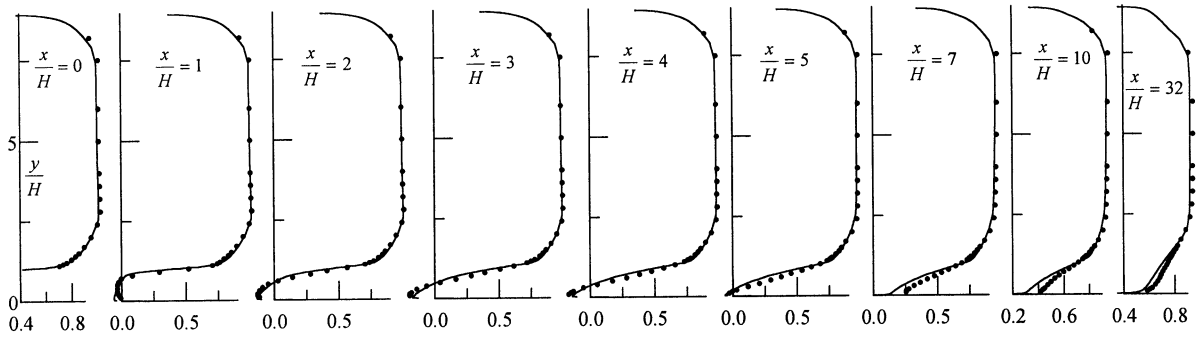

Fig.11. Mean velocity profiles U/U_0 in the backstep flow: — calculation, • experiment of Driver and Seegmiller (1985).

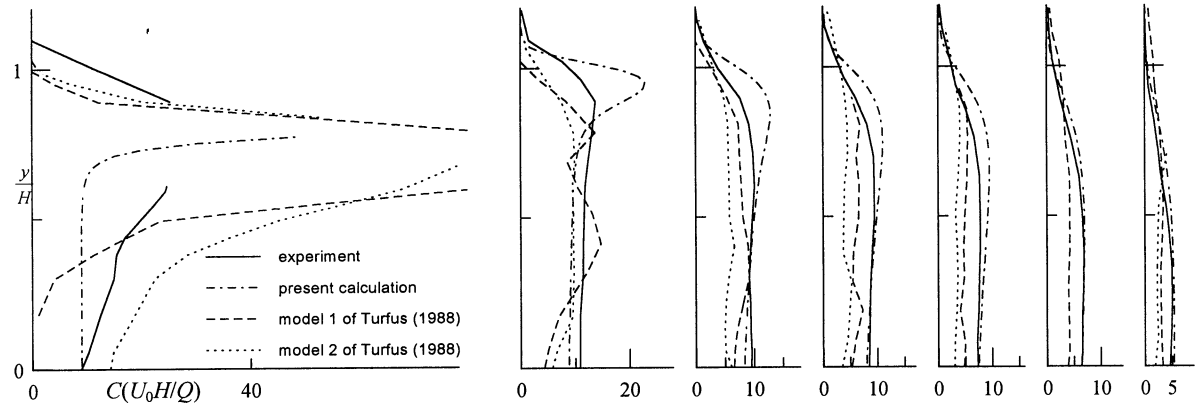

Figure 12. Mean concentration profiles in the backstep flow at x/H = 0; 1; 2; 2.5; 3; 4; 5 (source location 1).

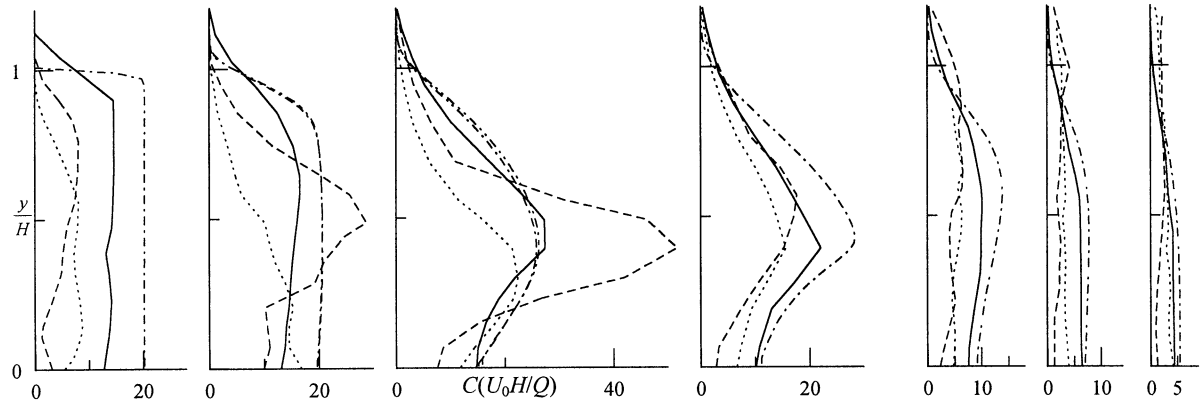

Figure 13. Mean concentration profiles in the backstep flow at x/H = 0; 1; 2; 2.5; 3; 4; 5 (source location 2).

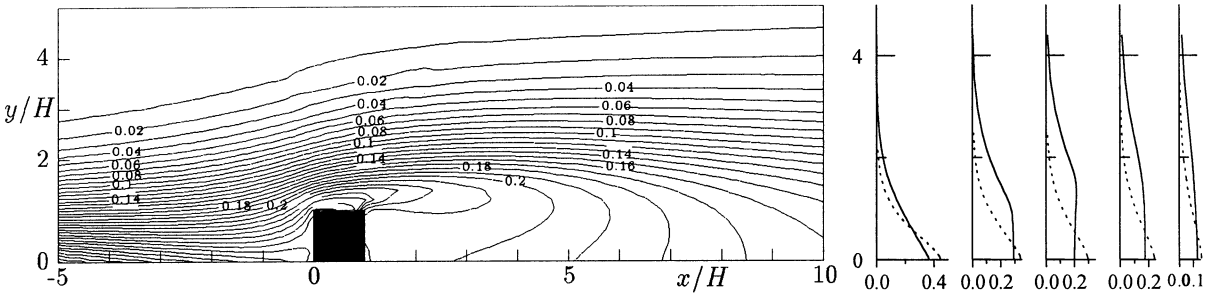

Figure 14. Calculated contour plots and profiles at x/H = -5; 0; 1; 5; 20 (— with obstacle, - - - without it) of normalized mean concentration C/C_0 in the boundary layer with obstacle (source is placed at x/H = -16 and y=0).